

Adjustable Visual Appearance for Generalizable Novel View Synthesis

Josef Bengtson¹
bjosef@chalmers.se

David Nilsson¹
david.nilsson@chalmers.se

Che-Tsung Lin¹
chetsung@chalmers.se

Marcel Büsching²
busching@kth.se

Fredrik Kahl¹
fredrik.kahl@chalmers.se

¹ Computer Vision Group, Chalmers
University of Technology

² KTH Royal Institute of Technology

Abstract

We present a generalizable novel view synthesis method where it is possible to modify the visual appearance of rendered views to match a target weather or lighting condition. Our method is based on a generalizable transformer architecture, trained on synthetically generated scenes under different appearance conditions. This allows for rendering novel views in a consistent manner of 3D scenes that were not included in the training set, along with the ability to (i) modify their appearance to match the target condition and (ii) smoothly interpolate between different conditions. Experiments on both real and synthetic scenes are provided including both qualitative and quantitative evaluations. Please refer to our project page for video results: <https://ava-nvs.github.io>

1 Introduction

The field of novel view synthesis has seen rapid progress in the last few years after the success of Neural Radiance Fields (NeRFs) [22] and follow-up works [10, 32, 48]. A desired quality for these types of 3D scene representations is to be able to disentangle different scene properties from each other, for instance, being able to change the visual appearance without changing the content of the scene. There exist some works in this direction [21, 36], but they are limited to interpolating between *observed* visual appearances of the 3D scene, thus requiring having images of the scene with the desired visual appearance. In contrast, we develop a method that is able to generalize to 3D scenes not used in training, and that thus can adjust the appearance of a scene without having access to any images of that scene at the target visual appearance, see Fig. 1.

For traditional NeRF-based methods, the properties of the 3D scene are encoded in the weights of a multilayer perceptron (MLP), so each trained model is exclusive to that particular scene. A main challenge is thus that an separate optimization process has to be performed

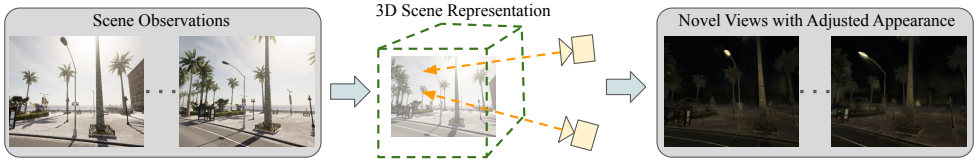


Figure 1: Given views in one weather and lighting condition, we want to generate novel views of the given scene with adjusted visual appearance corresponding to a target condition.

for each individual scene. One approach to handle this is to find ways to improve the efficiency of the training process [19, 23, 43]. A different approach is to avoid per-scene training and instead train cross-scene generalizable methods [6, 20, 35, 42, 47], which are able to synthesize novel views of a scene given just images and corresponding camera poses, and do not require expensive scene-specific optimization.

We present a generalizable novel view generation method which allows for changing the visual appearance of a scene while ensuring multi-view consistency. For this we build upon Generalizable NeRF Transformer (GNT) [35], a transformer [39] based novel view synthesis method. Specifically, we introduce a latent appearance variable to enable control of the visual appearance of rendered views. By using a generalizable NeRF model and this latent appearance variable, we are able to render novel views and change the appearance of scenes which are not seen when training our model without the need for observations of the scene at the target appearance.

In summary our main contributions are:

- We introduce a method that allows for changing the appearance of a novel scene by using a latent appearance variable conditioned on a target visual appearance.
- We propose a novel loss function which is designed to align the views rendered with a target appearance to the scene observed in that target condition, which enables jointly learning novel view synthesis and appearance change.
- We create a synthetic dataset containing urban scenes, with each scene available at four different diverse weather and lighting conditions. The dataset is used for training our model at visual appearance change and enables quantitative evaluation. The dataset will be made publicly available.

Limitations. Our work is restricted to realistic weather and lighting conditions, and we do not consider arbitrary appearance changes. Furthermore, our novel view synthesis is limited to the performance of the neural rendering method we base our method on.

2 Related work

Here we will review progress on NeRFs, focusing on works related to generalizable novel view synthesis. We will then review 2D style transfer methods and stylizing NeRFs methods.

Neural Radiance Fields. NeRFs [22] synthesize consistent and photo-realistic novel views of a scene, by representing each scene as a continuous 5D radiance field parameterized by an MLP mapping 3D positions and 2D viewing directions to volume densities and view-dependent emitted radiances. Views are synthesized by querying points along camera rays and map the output colors and densities into RGB values. There have been several works improving NeRFs further, e.g. to improve efficiency of the training process [19, 24, 43] and enable handling a low number of input views [18, 24, 47].

Generalizable Novel View Synthesis. The original NeRF methodology is constrained to training a neural network for representing a single scene, which requires a time-consuming optimization process performed from scratch for each new scene, without leveraging any prior knowledge. Methods for generalized neural rendering address this limitation by training across multiple scenes, enabling the learning of a general understanding of how to utilize source observations to synthesize novel views of the scene. Earlier methods such as [8, 47] use a multilayer perceptron (MLP) conditioned on feature vectors extracted from the source images to predict color and radiance values which are aggregated with volumetric rendering. To enhance generalization capabilities and rendering quality, recent approaches have incorporated transformer-based architectures [11, 39] for feature aggregation from the source images [20, 42], feature aggregation along the camera ray [44], and even for the entire rendering pipeline [26, 29, 33, 34, 35]. While these methods have demonstrated impressive rendering quality, they are currently incapable of modifying the appearance of the rendered views.

2D Style Transfer. Advances on 2D style transfer have largely been driven by the success of GANs [40]. Pix2pix[42] and Pix2pix-HD[45] are two prominent methods that provide visually-plausible images if paired training data is available, i.e., one image in the source condition and the corresponding image in the target. CyEDA[9] is an unpaired method that uses cycle-object edge consistency for achieving better image-object consistency.

More recently, diffusion models [8, 14, 51] have achieved better results in image-generation. The Instruct-pix2pix[4] method combined a text-to-image model (Stable Diffusion [27]) and a language model (GPT-3)[5] to enable instruction-based style transfer. Although the images translated by these 2D methods are realistic individually, temporal consistency is not ensured when the input images come from a sequence of consecutive images. We will experimentally compare our results with 2D style transfer methods.

Visual Appearance Change for NeRF Models. Prior work to enable changing the visual appearance of a NeRF model [21, 36] builds on Generative Latent Optimization (GLO) [3], where each image is assigned to an appearance embedding vector. This embedding vector is included as input to the part of the NeRF network for colors, enabling it to effect the visual appearance but not the geometry, and it is optimized alongside the NeRF model parameters. In [21] they choose a low dimensionality for these embeddings to find a continuous space, allowing for smooth interpolation between lighting conditions. One limitation with this approach is that it only allows for interpolation between already seen lighting conditions for a given scene, requiring access of images of that scene at both lighting conditions as input. In contrast, our method is a generalizable method that does not require images at both lighting conditions as input when rendering novel views.

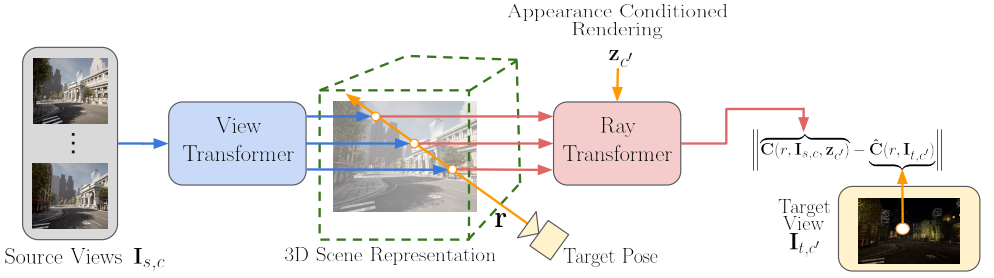


Figure 2: Overview of our method for changing visual appearance of synthesized novel views. A target view direction is chosen and camera rays \mathbf{r} are cast and the corresponding source views $I_{s,c}$ are used to generate a scene representation. A latent appearance variable $\mathbf{z}_{c'}$ is included with the goal of adapting the appearance of the rendered image to match the target view. If the target view is at a different weather or daylight conditions ($c \neq c'$) then this means adapting the visual appearance to match that found in the target view $I_{t,c'}$ instead of the visual appearance of the source views $I_{s,c}$.

Stylized NeRFs. Another line of research is to change the style of a NeRF model based on a given style prompt [13, 15, 16] typically given in the form of a reference image. More recent works [40, 41] use the joint language-image embedding space of the CLIP model [25] to enable specifying the desired style using a text prompt. Most of these methods are limited to only changing the color output, but not densities in the NeRF models and are thus unable to adapt the geometry of the scene. An exception to this is NeRF-Art [41], where geometry changes are performed. These methods are all based on per-scene NeRF models and not generalizable NeRF methods. They also focus on performing artistic style changes and have thus not been specifically trained and evaluated on realistic appearance changes such as differences in weather or lighting.

3 Method

We present our proposed method for novel view synthesis of a scene while changing the visual appearance. We start by giving an overview of Generalizable NeRF Transformer (GNT) [25] and then describe our method for adjusting the visual appearance of synthesized views, a long with the loss term we introduce.

3.1 Basics of GNT

GNT utilizes a two-stage transformer based architecture that allows for efficient novel view synthesis from source views. The first stage is a *view transformer* that aggregates information from neighbouring views while using epipolar geometry as an inductive bias. The second stage is a *ray transformer* that performs a learnable ray-based rendering based on the feature vectors generated by the *view transformer* along points on a camera ray.

View Transformer. The internal representation of the method is a coordinate aligned feature field $\mathcal{F} : (\mathbf{x}, \theta) \rightarrow \mathbf{f} \in \mathbb{R}^d$ that maps a 3D position \mathbf{x} and viewing direction θ to a feature vector \mathbf{f} , computed by the *view transformer*. Firstly each source view is encoded



Figure 3: Top: Input images generated in CARLA [9]. Bottom: Images generated by our method, where images from one condition are given as input along with latent appearance variable corresponding to another condition. We can see that our method is able to change the overall visual appearance of the images to match the desired condition, while also making local changes such as turning on a lamp when going from day to night or adding sunlight reflection on windows when going from day to evening. We also observe that going from day to night is more challenging, leading to blurriness and loss of detail.

to a feature map using a U-Net [28] Image Encoder $\mathbf{F}_i = \text{U-Net}(\mathbf{I}_i)$. To obtain the feature representation corresponding to a 3D point \mathbf{x} , the point is projected to every source image via the camera projections $\Pi_i(\mathbf{x})$, and then the corresponding feature values are calculated by interpolating the image-aligned feature map at the projected point. The *view transformer* is then used to combine all these feature vectors through attention as

$$\mathcal{F}(\mathbf{x}, \theta) = \text{View-Transformer}(\mathbf{F}_1(\Pi_1(\mathbf{x}), \theta), \dots, \mathbf{F}_N(\Pi_N(\mathbf{x}), \theta)). \quad (1)$$

Ray Transformer. The *ray transformer* aggregates information along a given camera ray by performing attention between feature values $\mathbf{f}_i = \mathcal{F}(\mathbf{x}_i, \theta)$, along the ray. The GNT pipeline consists of stacking several view and ray transformer blocks, which iteratively refines the feature field by first aggregating information from source views with the *view transformer* and then accumulating the information along the camera ray with the *ray transformer*. The final *ray transformer* then computes the RGB value $\mathbf{C}(\mathbf{r})$ corresponding to a camera ray $\mathbf{r} = (\mathbf{o}, \mathbf{d})$ by feeding the sequence of $\{\mathbf{f}_1, \dots, \mathbf{f}_M\}$ into the *ray transformer*, performing mean pooling over all predicted tokens, and mapping the pooled feature vector to RGB via an MLP as

$$\mathbf{C}(\mathbf{r}) = \text{MLP} \circ \text{Mean} \circ \text{Ray-Transformer}(\mathcal{F}(\mathbf{o} + t_1 \mathbf{d}, \theta), \dots, \mathcal{F}(\mathbf{o} + t_M \mathbf{d}, \theta)). \quad (2)$$

This enables training the method using the standard color prediction loss term commonly used by NeRFs.

The attention values from the ray transformer correspond to the importance of each feature vector \mathbf{f}_i along the ray to form the image, reflecting point-to-point based occlusion and visibility. It is thus the attention scores that determine the geometry of the rendered scenes, filling a similar role as the opacity in a traditional NeRF method.



Figure 4: Comparing our method with applying 2D style transfer on rendered images. Our method is able to drastically change appearance while preserving scene content, and gives multi-view consistent renderings. We observe that since Instruct-pix2pix[10] is not trained on our specific dataset it does not change the scene appearance to correspond to the visual appearance described by our night condition. Instruct-pix2pix and pix2pix-HD give inconsistent views, while CyEDA gives significantly more consistent results, as seen in Tab. 3.

3.2 Adjusting Visual Appearance

To change the visual appearance of rendered views to match a target appearance, we propose to introduce a latent appearance variable $\mathbf{z}_{c'}$ as an additional input to the *ray transformer*, with the goal of conditioning the rendering based on the target appearance. The full proposed architecture can be seen in Fig. 2.

The latent variable should correspond to a predefined appearance condition and the value for each condition is jointly optimized with the rest of the network. Since our goal is to change the visual appearance we include $\mathbf{z}_{c'}$ so that the geometry is kept unchanged. To ensure this it is used to update the value-tokens in the *ray transformer* while keeping the attention values unchanged, i.e.,

$$V_{c'} = f_z \left(\begin{bmatrix} V \\ \mathbf{z}_{c'} \end{bmatrix} \right), \quad (3)$$

where f_z is a single layer MLP that takes in the original value tokens V and generates updated value tokens $V_{c'}$ that have been updated based on the latent appearance variable $\mathbf{z}_{c'}$.

This enables computing a visual appearance change based loss term,

$$\mathcal{L}_{appearance} = \left\| \mathbf{C}(r, \mathbf{I}_{s,c}, \mathbf{z}_{c'}) - \hat{\mathbf{C}}(r, \mathbf{I}_{t,c'}) \right\|_2^2. \quad (4)$$

When inputting source views $\mathbf{I}_{s,c}$ from condition c together with the latent appearance variable $\mathbf{z}_{c'}$ corresponding to condition c' then the predicted color should match the ground truth color for the corresponding target images $\mathbf{I}_{t,c'}$. If the visual appearance of the target image $\mathbf{I}_{t,c}$ corresponds to that of the source images $\mathbf{I}_{s,c}$ then this becomes a traditional reconstruction



Figure 5: Gradually changing visual appearance by interpolating between latent appearance variables corresponding to day and night, respectively. The first row corresponds to latent variables generated with a given structure, enforcing that the evening condition lies in between day and night in the latent space, and the second row corresponds to a learned latent variable with no enforced structure. We observe that the model is able to smoothly interpolate between two conditions, generating plausible intermediate visual appearances. Comparing the two approaches we observe that the synthesized day-to-night-transformed images are very similar, but designing the latent space so that the interpolation goes through the evening condition leads to more realistic lighting changes in the interpolated views, giving the appearance of a sunset. Additional results for interpolation can be seen in the video on the [project page](#).

loss,

$$\mathcal{L}_{rec} = \left\| \mathbf{C}(r, I_{s,c}, \mathbf{z}_c) - \hat{\mathbf{C}}(r, \mathbf{I}_{t,c}) \right\|_2^2. \quad (5)$$

The final loss term is then acquired by combining these two loss terms,

$$\mathcal{L} = \mathcal{L}_{rec} + \mathcal{L}_{appearance}. \quad (6)$$

Rendering images with changed visual appearance is done by computing $\mathbf{C}(r, I_{s,c}, \mathbf{z}_{c'})$ for all pixels in an image, giving as input source views from one condition and a latent variable $\mathbf{z}_{c'}$ corresponding to the desired target condition.

4 Experiments

Qualitative and quantitative experiments are performed to test our method’s ability to adapt the visual appearance of real and synthetic scenes that have not been seen during training.

Dataset. The used dataset is generated using CARLA [1], an Unreal Engine 4 based open-source simulator for autonomous driving research. CARLA enables generating synthetic images within a simulated city environment along with their ground truth camera poses. Additionally, weather and lighting conditions can easily be changed.

For these experiments four conditions were defined, corresponding to *night*, *day*, *rain* and *evening*. A scene in the context of this simulated city was defined as a sequence of 10 observations taken along a road, with small pose differences between images. With four

Table 1: Comparison of similarity of rendered views for our method with ground truth images for different combinations of weather and lighting conditions (**PSNR**↑ | **SSIM**↑ | **LPIPS**↓). The values along the diagonal correspond to novel view synthesis without appearance change.

	From Day	From Night	From Evening	From Rain
Into Day	23.9 0.77 0.60	15.3 0.56 0.62	16.7 0.64 0.61	15.7 0.59 0.60
Into Night	21.0 0.56 0.55	27.4 0.68 0.57	20.7 0.54 0.55	21.2 0.57 0.55
Into Evening	24.1 0.75 0.58	20.0 0.62 0.57	25.4 0.76 0.58	21.4 0.69 0.57
Into Rain	23.4 0.71 0.58	21.7 0.66 0.57	21.3 0.69 0.56	26.8 0.78 0.58

Table 2: Quantitative results on CARLA [9] generated evaluation scenes, comparing to applying 2D style transfer methods on views rendered without appearance change (**PSNR**↑ | **SSIM**↑ | **LPIPS**↓). Best results for each combination of conditions is **highlighted**. Pix2pix-HD is the only of these methods trained in a way directly comparable to our method, which needs to be taken into account when comparing performance with the other two methods.

	Instruct-pix2pix [9]	CyEDA[9]	pix2pix-HD[9]	Ours
Day to Night	15.9 0.34 0.58	17.9 0.32 0.56	19.7 0.36 0.57	21.0 0.56 0.55
Day to Evening	14.3 0.53 0.65	18.8 0.40 0.59	18.4 0.35 0.60	24.1 0.75 0.58
Day to Rain	14.1 0.53 0.64	20.0 0.67 0.58	19.7 0.53 0.58	23.4 0.71 0.58
Night to Day	11.5 0.46 0.65	11.7 0.47 0.62	13.8 0.40 0.63	15.3 0.56 0.62
Evening to Day	8.7 0.34 0.67	13.7 0.59 0.64	15.3 0.46 0.62	16.7 0.64 0.61
Rain to Day	13.4 0.52 0.64	12.3 0.53 0.63	13.94 0.43 0.63	15.7 0.59 0.60

different conditions this led to a total of 40 images per scene. All generated images are 800×600 pixels. The CARLA map was split into two regions, one was used to generate 145 training scenes, and the other region was used to generate 38 evaluation scenes, ensuring diversity between training and evaluation. This dataset alongside the code will be made publicly available. We also show qualitative examples using the Spaces dataset [10] to see how our method generalizes to real data.

Implementation. The model was initialized with weights from a GNT network pretrained on a combination of synthetic and real data, as specified in [6]. The model was trained to perform visual appearance change using the 145 training scenes, using the proposed loss term (6) for 50 000 iterations. For our case with four weather and lighting conditions, we represented each condition as a fix 2D-coordinate, placing them such that the evening condition is in between day and night. These fixed 2D coordinates were fed through a small fully-connected network to generate \mathbf{z}_c , a learned latent representation of dimension d for each condition. We also compared this to the case of just introducing the latent variable directly as a learnable vector of dimension d , without enforcing any structure on the latent space, a comparison of the two approaches can be seen in Fig. 5. The latent dimension $d = 136$ was chosen for the performed experiments, further details regarding this choice of d and the two setups for generating \mathbf{z}_c can be found in appendix A. The remaining parameters were selected as in the GNT paper [6].

Discussion. Our trained model is evaluated on the 38 evaluation scenes not seen during training. The only required input is a set of images with corresponding poses and the method can then generate novel views of that scene with visual appearance changed to match one of the four given weather and lighting conditions. We show several qualitative examples.

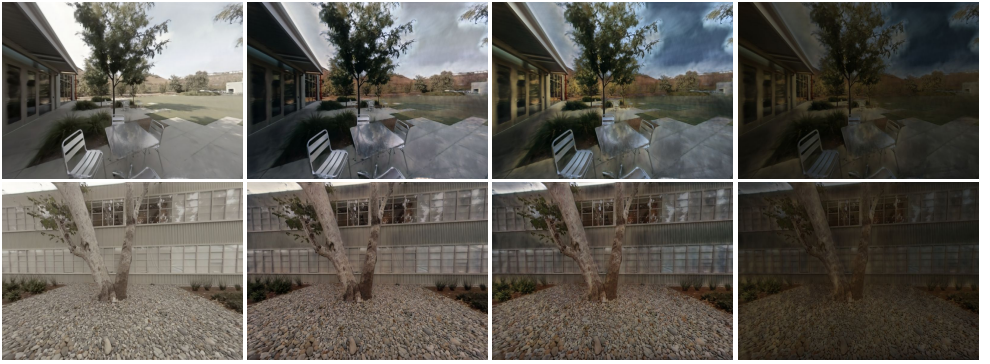


Figure 6: Visual appearance change applied on two scenes from the Spaces dataset [14]. The left column shows views rendered at the original condition, the subsequent columns show interpolation between day and night. We see that our method is able to change the appearance of real scenes, even when only being trained on changing the appearance of synthetic scenes.

Fig. 3 shows that our method is able to change the visual appearance of images to match a target weather and lighting condition, and Fig. 4 shows comparison with three different 2D style transfer methods. It also becomes possible to interpolate between two latent variables corresponding to different conditions, by defining $\mathbf{z}_\alpha = \alpha \mathbf{z}_c + (1 - \alpha) \mathbf{z}_{c'}$ for $\alpha \in [0, 1]$. In Fig. 5 we observe that this enables getting realistic intermediate visual appearances that are not included in the original images. The model trained on appearance change of synthetic scenes can also be applied to change appearance of real scenes [14], as seen in Fig. 6 where we can see realistic appearance changes even though the model is not trained on that data.

We now show quantitative results based on the three performance measures PSNR, SSIM [46] and LPIPS [49]. The images with changed appearance are evaluated against the corresponding ground truth images for the target weather and lighting condition. In Table 1 we show how our method performs on all possible pairs of source and target conditions. Using the same source and target conditions corresponds to novel view synthesis without appearance change, which as expected gives better metrics, but for some combinations the gap is small, e.g. comparing Day into Evening with Evening into Evening. In Table 2 we compare our method with several 2D style transfer methods. We see that our method outperforms the 2D-methods on PSNR and SSIM for all combinations, while giving competitive results for LPIPS. We observe that performance varies for the different conditions, and that adapting images from another condition into day is the most challenging, while transforming from day gives significantly higher performance for all methods.

Additionally, we show two consistency metrics [20] in Table 3. If (x_1, \dots, x_n) and (y_1, \dots, y_n) are two image sequences rendered from the same pose sequences, we define $\text{tOF} = \|\text{OF}(y_{t+1}, y_t) - \text{OF}(x_{t+1}, x_t)\|_1$, where OF is the optical flow computed via RAFT [67] and $\text{tLP} = \|\text{LPIPS}(y_{t+1}, y_t) - \text{LPIPS}(x_{t+1}, x_t)\|_1$. The metrics are low if the reference images and the rendered images yield similar optical flow and similar changes in LPIPS, which is assumed to correspond to a consistent rendering. We see that our method and CyEDA significantly outperform the other 2D style transfer baselines.

Table 3: Comparison of the consistency of the novel view rendering with 2D-methods (tOF↓ | tLP↓ [□]). We see that our method and CyEDA significantly outperform the other two methods. Please see the video on the [project page](#) for visual comparison of the rendering consistency for the different methods.

	Instruct-pix2pix [□]	CyEDA[□]	pix2pix-HD[□]	Ours
Day to Night	1.62 0.123	1.56 0.025	2.59 0.147	1.44 0.026
Day to Rain	1.45 0.088	0.96 0.022	1.60 0.030	0.97 0.013
Day to Evening	1.37 0.121	1.21 0.115	1.58 0.169	1.10 0.035
Night to Day	1.48 0.092	1.25 0.032	2.49 0.078	1.25 0.032

5 Conclusions

We present a transformer based generalizable novel view synthesis method that allows for visual appearance changes. This is achieved by introducing a latent appearance variable that is used to change the visual appearance to match a given weather and lighting condition while keeping the structure of the scene unchanged. We present experiments that show that this method is able to change the visual appearance of both synthetic and real scenes that have not seen during training, to match a specified weather and lighting condition. The generated latent variables also make it possible to smoothly interpolate between different weather and lighting conditions. Compared to 2D style transfer methods, our method is view consistent by design.

6 Acknowledgments

This work was fully supported by the Wallenberg AI, Autonomous Systems and Software Program (WASP) funded by the Knut and Alice Wallenberg Foundation.

References

- [1] Jonathan T. Barron, Ben Mildenhall, Matthew Tancik, Peter Hedman, Ricardo Martin-Brualla, and Pratul P. Srinivasan. Mip-nerf: A multiscale representation for anti-aliasing neural radiance fields. *ICCV*, 2021.
- [2] Jing Chong Beh, Kam Woh Ng, Jie Long Kew, Che-Tsung Lin, Chee Seng Chan, Shang-Hong Lai, and Christopher Zach. Cyeda: Cycle-object edge consistency domain adaptation. In *2022 IEEE International Conference on Image Processing (ICIP)*, pages 2986–2990. IEEE, 2022.
- [3] Piotr Bojanowski, Armand Joulin, David Lopez-Paz, and Arthur Szlam. Optimizing the latent space of generative networks. *ICML*, 2018.
- [4] Tim Brooks, Aleksander Holynski, and Alexei A. Efros. Instructpix2pix: Learning to follow image editing instructions. In *CVPR*, 2023.
- [5] Tom Brown, Benjamin Mann, Nick Ryder, Melanie Subbiah, Jared D Kaplan, Prafulla Dhariwal, Arvind Neelakantan, Pranav Shyam, Girish Sastry, Amanda Askell, et al. Language models are few-shot learners. *Advances in neural information processing systems*, 33:1877–1901, 2020.

- [6] Anpei Chen, Zexiang Xu, Fuqiang Zhao, Xiaoshuai Zhang, Fanbo Xiang, Jingyi Yu, and Hao Su. Mvsnerf: Fast generalizable radiance field reconstruction from multi-view stereo. In *Proceedings of the IEEE/CVF International Conference on Computer Vision (ICCV)*, pages 14124–14133, October 2021.
- [7] Mengyu Chu, You Xie, Jonas Mayer, Laura Leal-Taixé, and Nils Thuerey. Learning temporal coherence via self-supervision for gan-based video generation. *ACM Transactions on Graphics (TOG)*, 39(4):75–1, 2020.
- [8] Prafulla Dhariwal and Alexander Nichol. Diffusion models beat gans on image synthesis. *Advances in Neural Information Processing Systems*, 34:8780–8794, 2021.
- [9] Alexey Dosovitskiy, German Ros, Felipe Codevilla, Antonio Lopez, and Vladlen Koltun. CARLA: An open urban driving simulator. In *Proceedings of the 1st Annual Conference on Robot Learning*, pages 1–16, 2017.
- [10] Alexey Dosovitskiy, Lucas Beyer, Alexander Kolesnikov, Dirk Weissenborn, Xiaohua Zhai, Thomas Unterthiner, Mostafa Dehghani, Matthias Minderer, Georg Heigold, Sylvain Gelly, Jakob Uszkoreit, and Neil Houlsby. An Image is Worth 16x16 Words: Transformers for Image Recognition at Scale. In *International Conference on Learning Representations (ICLR)*, 2022. URL <https://openreview.net/forum?id=YicbFdNTTy>.
- [11] John Flynn, Michael Broxton, Paul Debevec, Matthew DuVall, Graham Fyffe, Ryan Overbeck, Noah Snavely, and Richard Tucker. Deepview: View synthesis with learned gradient descent. In *Proceedings of the IEEE/CVF Conference on Computer Vision and Pattern Recognition (CVPR)*, June 2019.
- [12] Ian Goodfellow, Jean Pouget-Abadie, Mehdi Mirza, Bing Xu, David Warde-Farley, Sherjil Ozair, Aaron Courville, and Yoshua Bengio. Generative adversarial networks. *Communications of the ACM*, 63(11):139–144, 2020.
- [13] Jiatao Gu, Lingjie Liu, Peng Wang, and Christian Theobalt. StyleNeRF: A style-based 3d aware generator for high-resolution image synthesis. In *International Conference on Learning Representations*, 2022. URL <https://openreview.net/forum?id=iUuzzTMUw9K>.
- [14] Jonathan Ho, Ajay Jain, and Pieter Abbeel. Denoising diffusion probabilistic models. *Advances in Neural Information Processing Systems*, 33:6840–6851, 2020.
- [15] Xun Huang and Serge Belongie. Arbitrary style transfer in real-time with adaptive instance normalization. In *Proceedings of the IEEE International Conference on Computer Vision (ICCV)*, Oct 2017.
- [16] Yi-Hua Huang, Yue He, Yu-Jie Yuan, Yu-Kun Lai, and Lin Gao. Stylizednerf: Consistent 3d scene stylization as stylized nerf via 2d-3d mutual learning. In *Computer Vision and Pattern Recognition (CVPR)*, 2022.
- [17] Phillip Isola, Jun-Yan Zhu, Tinghui Zhou, and Alexei A Efros. Image-to-image translation with conditional adversarial networks. In *Conference on Computer Vision and Pattern Recognition (CVPR)*, pages 1125–1134, 2017.

- [18] Ajay Jain, Matthew Tancik, and Pieter Abbeel. Putting nerf on a diet: Semantically consistent few-shot view synthesis. In *Proceedings of the IEEE/CVF International Conference on Computer Vision (ICCV)*, pages 5885–5894, October 2021.
- [19] Andreas Kurz, Thomas Neff, Zhaoyang Lv, Michael Zollhöfer, and Markus Steinberger. Adanerf: Adaptive sampling for real-time rendering of neural radiance fields. In *European Conference on Computer Vision (ECCV)*, 2022.
- [20] Yuan Liu, Sida Peng, Lingjie Liu, Qianqian Wang, Peng Wang, Theobalt Christian, Xiaowei Zhou, and Wenping Wang. Neural rays for occlusion-aware image-based rendering. In *CVPR*, 2022.
- [21] Ricardo Martin-Brualla, Noha Radwan, Mehdi S. M. Sajjadi, Jonathan T. Barron, Alexey Dosovitskiy, and Daniel Duckworth. Nerf in the wild: Neural radiance fields for unconstrained photo collections. In *Proceedings of the IEEE/CVF Conference on Computer Vision and Pattern Recognition (CVPR)*, pages 7210–7219, June 2021.
- [22] Ben Mildenhall, Pratul P. Srinivasan, Matthew Tancik, Jonathan T. Barron, Ravi Ramamoorthi, and Ren Ng. Nerf: Representing scenes as neural radiance fields for view synthesis. In *ECCV*, 2020.
- [23] Thomas Müller, Alex Evans, Christoph Schied, and Alexander Keller. Instant neural graphics primitives with a multiresolution hash encoding. *ACM Trans. Graph.*, 41(4): 102:1–102:15, July 2022. doi: 10.1145/3528223.3530127. URL <https://doi.org/10.1145/3528223.3530127>.
- [24] Michael Niemeyer, Jonathan T. Barron, Ben Mildenhall, Mehdi S. M. Sajjadi, Andreas Geiger, and Noha Radwan. Regnerf: Regularizing neural radiance fields for view synthesis from sparse inputs. In *Proceedings of the IEEE/CVF Conference on Computer Vision and Pattern Recognition (CVPR)*, pages 5480–5490, June 2022.
- [25] Alec Radford, Jong Wook Kim, Chris Hallacy, Aditya Ramesh, Gabriel Goh, Sandhini Agarwal, Girish Sastry, Amanda Askell, Pamela Mishkin, Jack Clark, Gretchen Krueger, and Ilya Sutskever. Learning transferable visual models from natural language supervision. In Marina Meila and Tong Zhang, editors, *Proceedings of the 38th International Conference on Machine Learning*, volume 139 of *Proceedings of Machine Learning Research*, pages 8748–8763. PMLR, 18–24 Jul 2021. URL <https://proceedings.mlr.press/v139/radford21a.html>.
- [26] Jeremy Reizenstein, Roman Shapovalov, Philipp Henzler, Luca Sbordone, Patrick Labatut, and David Novotny. Common objects in 3d: Large-scale learning and evaluation of real-life 3d category reconstruction. In *Proceedings of the IEEE/CVF International Conference on Computer Vision (ICCV)*, pages 10901–10911, October 2021.
- [27] Robin Rombach, Andreas Blattmann, Dominik Lorenz, Patrick Esser, and Björn Ommer. High-resolution image synthesis with latent diffusion models. In *Proceedings of the IEEE/CVF Conference on Computer Vision and Pattern Recognition*, pages 10684–10695, 2022.
- [28] O. Ronneberger, P. Fischer, and T. Brox. U-net: Convolutional networks for biomedical image segmentation. In *Medical Image Computing and*

- Computer-Assisted Intervention (MICCAI)*, volume 9351 of *LNCS*, pages 234–241. Springer, 2015. URL <http://lmb.informatik.uni-freiburg.de/Publications/2015/RFB15a>. (available on arXiv:1505.04597 [cs.CV]).
- [29] Mehdi S.M. Sajjadi, Henning Meyer, Etienne Pot, Urs Bergmann, Klaus Greff, Noha Radwan, Suhani Vora, Mario Lucic, Daniel Duckworth, Alexey Dosovitskiy, Jakob Uszkoreit, Thomas Funkhouser, and Andrea Tagliasacchi. Scene Representation Transformer: Geometry-Free Novel View Synthesis Through Set-Latent Scene Representations. In *Proceedings of the IEEE/CVF Conference on Computer Vision and Pattern Recognition (CVPR)*, pages 6219–6228, 2022. doi: 10.1109/CVPR52688.2022.00613.
- [30] Torsten Sattler, Will Maddern, Carl Toft, Akihiko Torii, Lars Hammarstrand, Erik Stenborg, Daniel Safari, Masatoshi Okutomi, Marc Pollefeys, Josef Sivic, Fredrik Kahl, and Tomas Pajdla. Benchmarking 6DOF Outdoor Visual Localization in Changing Conditions. In *Conference on Computer Vision and Pattern Recognition (CVPR)*, 2018.
- [31] Jascha Sohl-Dickstein, Eric Weiss, Niru Maheswaranathan, and Surya Ganguli. Deep unsupervised learning using nonequilibrium thermodynamics. In *International Conference on Machine Learning*, pages 2256–2265. PMLR, 2015.
- [32] Pratul P. Srinivasan, Boyang Deng, Xiuming Zhang, Matthew Tancik, Ben Mildenhall, and Jonathan T. Barron. Nerv: Neural reflectance and visibility fields for relighting and view synthesis. In *CVPR*, 2021.
- [33] Mohammed Suhail, Carlos Esteves, Leonid Sigal, and Ameesh Makadia. Generalizable Patch-Based Neural Rendering. In *European Conference on Computer Vision (ECCV)*, pages 156–174, 2022. doi: 10.1007/978-3-031-19824-3_10.
- [34] Mohammed Suhail, Carlos Esteves, Leonid Sigal, and Ameesh Makadia. Light Field Neural Rendering. In *Proceedings of the IEEE/CVF Conference on Computer Vision and Pattern Recognition (CVPR)*, pages 8259–8269, 2022. doi: 10.1109/CVPR52688.2022.00809.
- [35] Mukund Varma T, Peihao Wang, Xuxi Chen, Tianlong Chen, Subhashini Venugopalan, and Zhangyang Wang. Is attention all that nerf needs? In *The Eleventh International Conference on Learning Representations*, 2023. URL <https://openreview.net/forum?id=xE-LtsE-xx>.
- [36] Matthew Tancik, Vincent Casser, Xincheng Yan, Sabeek Pradhan, Ben Mildenhall, Pratul P. Srinivasan, Jonathan T. Barron, and Henrik Kretschmar. Block-nerf: Scalable large scene neural view synthesis. In *Proceedings of the IEEE/CVF Conference on Computer Vision and Pattern Recognition (CVPR)*, pages 8248–8258, June 2022.
- [37] Zachary Teed and Jia Deng. Raft: Recurrent all-pairs field transforms for optical flow. In *Computer Vision—ECCV 2020: 16th European Conference, Glasgow, UK, August 23–28, 2020, Proceedings, Part II 16*, pages 402–419. Springer, 2020.
- [38] Carl Toft, Carl Olsson, and Fredrik Kahl. Long-term 3D Localization and Pose from Semantic Labellings. In *ICCV Workshops*, 2017.

- [39] Ashish Vaswani, Noam Shazeer, Niki Parmar, Jakob Uszkoreit, Llion Jones, Aidan N Gomez, Łukasz Kaiser, and Illia Polosukhin. Attention is All you Need. In *Neural Information Processing Systems (NIPS)*, pages 6000–6010, 2017. URL <https://proceedings.nips.cc/paper/2017/hash/3f5ee243547dee91fbd053c1c4a845aa-Abstract.html>.
- [40] Can Wang, Menglei Chai, Mingming He, Dongdong Chen, and Jing Liao. Clip-nerf: Text-and-image driven manipulation of neural radiance fields. In *Proceedings of the IEEE/CVF Conference on Computer Vision and Pattern Recognition (CVPR)*, pages 3835–3844, June 2022.
- [41] Can Wang, Ruixiang Jiang, Menglei Chai, Mingming He, Dongdong Chen, and Jing Liao. Nerf-art: Text-driven neural radiance fields stylization. *arXiv preprint arXiv:2212.08070*, 2022.
- [42] Dan Wang, Xinrui Cui, Septimiu Salcudean, and Z. Jane Wang. Generalizable neural radiance fields for novel view synthesis with transformer, 2022. URL <https://arxiv.org/abs/2206.05375>.
- [43] Huan Wang, Jian Ren, Zeng Huang, Kyle Olszewski, Menglei Chai, Yun Fu, and Sergey Tulyakov. R2l: Distilling neural radiance field to neural light field for efficient novel view synthesis. In *ECCV*, 2022.
- [44] Qianqian Wang, Zhicheng Wang, Kyle Genova, Pratul P. Srinivasan, Howard Zhou, Jonathan T. Barron, Ricardo Martin-Brualla, Noah Snavely, and Thomas Funkhouser. Ibrnet: Learning multi-view image-based rendering. In *Proceedings of the IEEE/CVF Conference on Computer Vision and Pattern Recognition (CVPR)*, pages 4690–4699, June 2021.
- [45] Ting-Chun Wang, Ming-Yu Liu, Jun-Yan Zhu, Andrew Tao, Jan Kautz, and Bryan Catanzaro. High-resolution image synthesis and semantic manipulation with conditional gans. In *Conference on Computer Vision and Pattern Recognition (CVPR)*, pages 8798–8807, 2018.
- [46] Zhou Wang, A.C. Bovik, H.R. Sheikh, and E.P. Simoncelli. Image quality assessment: from error visibility to structural similarity. *IEEE Transactions on Image Processing*, 13(4):600–612, 2004. doi: 10.1109/TIP.2003.819861.
- [47] Alex Yu, Vickie Ye, Matthew Tancik, and Angjoo Kanazawa. pixelnerf: Neural radiance fields from one or few images. In *Proceedings of the IEEE/CVF Conference on Computer Vision and Pattern Recognition (CVPR)*, pages 4578–4587, June 2021.
- [48] Kai Zhang, Gernot Riegler, Noah Snavely, and Vladlen Koltun. Nerf++: Analyzing and improving neural radiance fields. *arXiv preprint arXiv:2010.07492*, 2020. URL <http://arxiv.org/abs/2010.07492v2>.
- [49] Richard Zhang, Phillip Isola, Alexei A. Efros, Eli Shechtman, and Oliver Wang. The unreasonable effectiveness of deep features as a perceptual metric. In *2018 IEEE/CVF Conference on Computer Vision and Pattern Recognition*, pages 586–595, 2018. doi: 10.1109/CVPR.2018.00068.

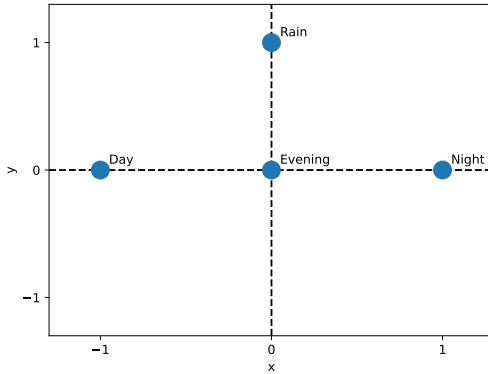


Figure 7: Chosen fixed 2D coordinates for each condition, ensuring that one passes through the evening condition when interpolating between day and night conditions. Rain is placed on a separate axis since it corresponds to appearance change not directly connected to daylight condition.

Appendix

In appendix A we describe and compare two different methods for generating latent variables. In appendix B we show additional qualitative results.

A Generating Latent Variables

We compare two different ways of learning latent appearance variables $\mathbf{z}_c \in \mathbb{R}^d$. One approach is to initialize a random d -dimensional vector for each condition and then include it as a learnable parameter that is optimized jointly with the rest of the model. For this case the latent variables are fully learned with no enforced structure.

Another approach is to enforce structure on the latent appearance variables by defining fixed 2D-coordinates c corresponding to each condition that are then passed through a small fully-connected network $f_z(c)$ to generate \mathbf{z}_c , where the parameters of this additional fully-connected network are learned jointly with the rest of the model. For our case with four weather and lighting conditions we define the fixed 2D-coordinates as,

$$c_{day} = \begin{bmatrix} -1 \\ 0 \end{bmatrix}, c_{evening} = \begin{bmatrix} 0 \\ 0 \end{bmatrix}, c_{rain} = \begin{bmatrix} 0 \\ 1 \end{bmatrix}, c_{night} = \begin{bmatrix} 1 \\ 0 \end{bmatrix}, \quad (7)$$

as seen in Fig. 7. The reason behind these placements is to get desired behavior when interpolating between two conditions. This placement ensures that the evening condition is passed through when interpolating between day and night conditions, and places rain on a separate axis since it corresponds to appearance change not directly connected to daylight condition. The fully connected network $f_z(c)$ takes in a 2D coordinate corresponding to a condition and outputs a latent appearance variable \mathbf{z}_c of dimension d . For the performed experiments we used $d = 136$, and two hidden layers of size 16 and 68 respectively. The choice of d was made after testing different values and observing that a higher dimension leads to better ability to handle local appearance changes such as turning on lamps and removing shadows, as seen in Fig. 8.

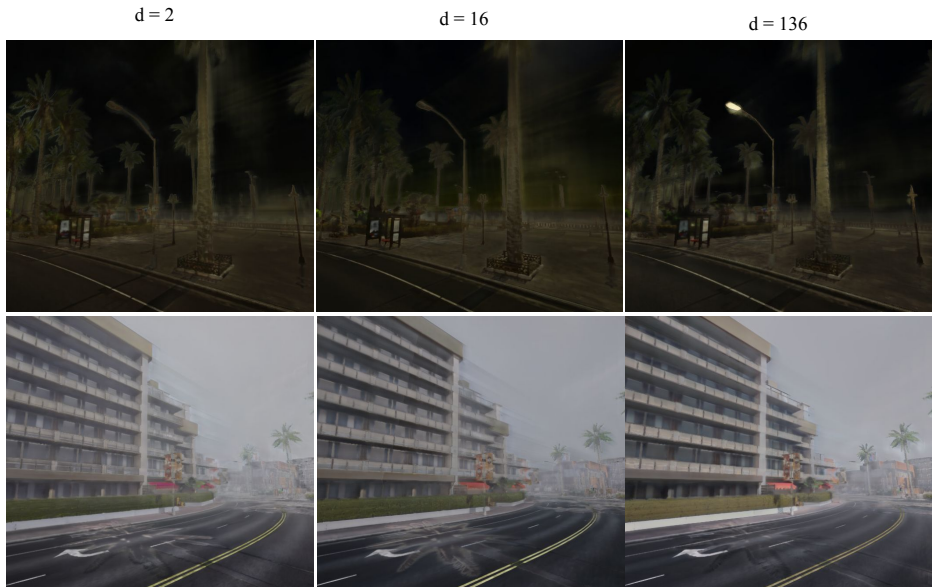


Figure 8: Qualitative comparison of rendered views with changed appearance for different sizes d of the latent appearance variable \mathbf{z}_c . We observe that a higher value of d leads to better local appearance changes in rendered views, such as turning on lamps and removing shadows.

Comparing performance metrics for learnable latent variables with no enforced structure in Table 4 with the ones in Table 1 where latent appearance variables with enforced structure are used, shows that both approaches for generating the latent variable \mathbf{z}_c give similar performance when changing appearance from one condition to another. However, enforcing a structure on the latent space leads to more realistic lighting effects when interpolating, as can be seen in Fig. 5. Based on this it was decided to use the latent appearance variable with enforced structure for our experiments.

B Additional Qualitative Results

We include additional figures showing the ability for our method to change the visual appearance of rendered views to match a target appearance. Figs. 9 and 10 show images generated by our method for additional combinations of weather and lighting conditions.

Table 4: Comparison of similarity of rendered views when using randomly initialized latent variables that are included as learnable parameters. Comparing with ground truth images for different combinations of weather and lighting conditions (**PSNR**↑ | **SSIM**↑ | **LPIPS**↓). The values along the diagonal correspond to novel view synthesis without appearance change.

	From Day	From Night	From Evening	From Rain
Into Day	23.3 0.76 0.61	15.3 0.56 0.61	16.4 0.61 0.60	15.9 0.61 0.61
Into Night	21.6 0.57 0.55	28.1 0.73 0.55	21.1 0.56 0.54	21.4 0.58 0.55
Into Evening	23.2 0.71 0.57	19.9 0.47 0.58	23.1 0.55 0.57	20.3 0.50 0.57
Into Rain	22.8 0.70 0.55	20.9 0.66 0.56	21.3 0.69 0.57	23.1 0.55 0.58



Figure 9: Changed visual appearance for going between Rain and Night conditions. Top: Input images generated in CARLA [9]. Bottom: Images generated by our method, where images from one condition are given as input along with a latent appearance variable corresponding to another condition.

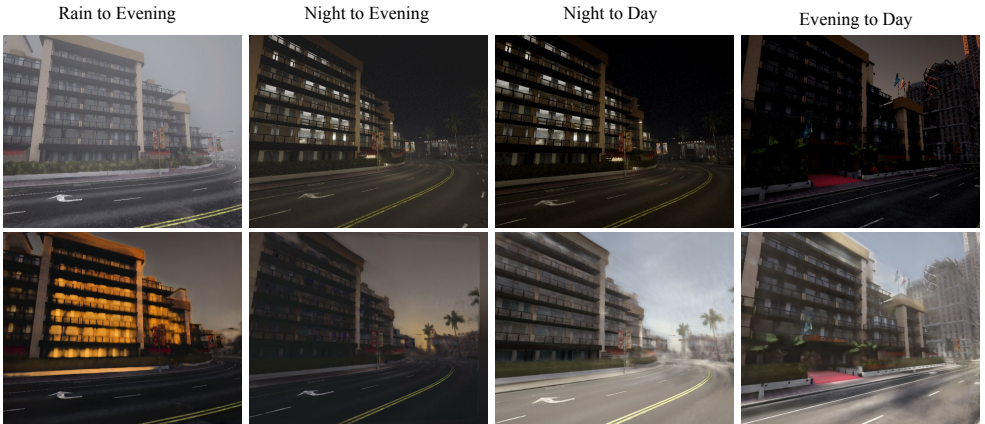


Figure 10: Changed appearance for buildings with many windows, showing that our method can handle effects such as adding sunlight reflection on windows and turning off interior lamps. Top: Input images generated in CARLA [9]. Bottom: Images generated by our method, where images from one condition are given as input along with a latent appearance variable corresponding to another condition.